Supporting Information

For

Imino−Phenolic–Azodye Appended Rhodamine as Primary Fluorescence "Off−On" Chemosensors for Tin (Sn^{4+}) in Solution and in Raw Cells and the Recognition of Sulphide by [AR-Sn]

Ajit Kumar Mahapatra*,[a] Saikat Kumar Manna,[a] Kalipada Maiti,[a] Rajkishor Maji,[a] Chitrangada Das Mukhopadhyay[b], Deblina Sarkar[c] and Tapan Kumar Mondal[c]

[a]Department of Chemistry and [b]Centre for Healthcare Science & Technology, Indian Institute of Engineering Science and Technology, Shibpur, Howrah – 711103, India.

[c]Department of Chemistry, Jadavpur University, Kolkata-700032, India.

Contents

1. EXPERIMENTAL DETAILS:

General Methods and Materials. All of the materials for synthesis were commercially available and used without further purification. Solutions of Li^+, Na^+, K^+, Sr^{2+}, Ba^{2+}, Cr^{3+}, Ca^{2+}, Al^{3+}, Fe^{3+}, Pb^{2+} and Sn^{4+} were prepared from chloride salts; solutions of Hg^{2+}, Cu^{2+}, Cd^{2+}, Fe^{2+}, Co^{2+}, Ni^{2+}, Mn^{2+}, Zn^{2+}, Mg^{2+} were prepared from perchlorate salts; solution of Ag^+ was prepared from nitrate salts and used immediately. For spectrophotometer measurements, EtOH (Spectrochem) and Elix Millipore water were used as solvents throughout all experiments. UV–visible spectra were recorded with a JASCO V530 spectrophotometer. Fluorescence spectra recorded with Photon Technology International (PTI-LPS-220B) spectrophotometer. FTIR spectra were recorded as KBr pellets using a JASCO FTIR spectrometer (model FTIR-460 plus). The ^1H and ^{13}C NMR spectra were recorded on Bruker–400 MHz spectrometer. Mass spectra were carried out using a Water's QTOF Micro YA 263 mass spectrometer. The ^1H NMR chemical shift values are expressed in ppm (δ) relative to $CHCl_3$ (δ = 7.25 ppm).

Solution of the probe **AR** in EtOH/H_2O (4:1, v/v) were 4.0×10^{-5} M, and those of metals in H_2O were 4.0×10^{-4} M. In titration experiments, each time a 4×10^{-5} M solution of **AR** was filled in a quartz optical cell of 1 cm optical path length, and the ion stock solutions were added into the quartz optical cell gradually by using a micropipette. During fluorometric titration, excitation was provided at 563 nm, and emission was collected from 572 to 680 nm.

Synthesis of 2: Rhodamine-B hydrazide (2) were synthesized according to literature methods. [1]

Synthesis of NAR. NAR has been synthesized by similar diazocoupling and condensation reactions starting from 2-formyl-1-naphthol instead of salicylaldehyde. ^{1}H NMR (400 MHz, $CDCl_3$, $Si(CH_3)_4$, J (Hz), δ(ppm)): 12.78 (1H, s, -OH), 9.05 (1H, s, -CH=N), 8.84 (1H, d, J=8.28 Hz), 8.42 (1H, d, J=8.36 Hz), 8.19 (2H, d, J=8.44 Hz), 7.99 (3H, t, J=8.48 Hz), 7.71(1H, s), 7.66 (1H, t, J=7.24 Hz), 7.51 (3H, m), 7.16 (1H, d, J=6.88 Hz), 6.52 (4H, dd, J= 2.28 & 8.84 Hz), 6.27(2H, dd, J= 2.24 & 2.28 Hz), 4.41 (2H, q, J=7.16 Hz), 3.32 (8H, q, J=7.00 Hz, -N$\underline{CH_2}CH_3$), 1.39 (3H, t, J= 6.00 Hz), 1.31 (12H, t, J= 7.00 Hz, -$NCH_2\underline{CH_3}$). TOF MS ES$^+$, m/z = 787.3596, calc. for $C_{48}H_{46}N_6O_5$ =786.9284.

Effect of pH: To study the practical applicability, the effects of pH on the fluorescence response of sensor **AR** to Sn^{4+} was investigated. As shown in Figure S15 the fluorescence responses of **AR** without and with Sn^{4+} ions as a function of pH . Experimental results show that for free **AR**, at acidic conditions (pH <5), an obvious off-on fluorescence appeared due to the formation of the open-ring state because of the strong protonation. In the pH range from 4.5 to 9.0, little fluorescence signal (excited at 563 nm) could be observed for free **AR**, suggesting that the molecules prefer the spirocyclic form. Upon the addition of Sn^{4+} ions, there was an obvious fluorescence off-on change of **AR** under different pH values and the pH-control emission measurements revealed that **AR** could respond to Sn^{4+} ions in the pH range from 5 to 9 with little changes of the fluorescent intensity, suggesting that the **AR** facilitates quantification of the concentration of Sn^{4+} ions in aqueous solution in a wide pH range. Considering that most samples for Sn^{4+} ions analysis were neutral, therefore, the media for Sn^{4+} ions quantification was then buffered at pH 7.

Cell Line and Cell Culture. In this work, RAW 264.7 macrophages were obtained from NCCS, Pune, India and maintained in DMEM containing 10% (v/v) fetal calf serum and antibiotics in a CO_2 incubator. Frozen Human colorectal carcinoma cell line HCT 116 (ATCC : CCL-247) were obtained from the American Type Culture Collection (Rockville, MD, USA) . All cell line were maintained in Dulbecco's modified Eagle's medium (DMEM, Sigma Chemical Co., St. Louis, MO, USA) supplemented with 10% fetal bovine serum (Invitrogen), penicillin (100 μg/mL), and streptomycin (100 μg/mL). Cells were initially propagated in 25 cm^2 tissue culture flask in an atmosphere of 5% CO_2 and 95% air at 37°C humidified air till 70- 80% confluency.

Confocal Imaging Study of Cells. For imaging studies, RAW 264.7, 1×10^{-5} cells in 150 μL of medium, were seeded on sterile Poly L lysine coated coverslip of 12 mm diameter kept in a sterile 35 mm covered Petri dish and incubated overnight in a CO_2 incubator at 37 °C. Next day, cells were washed with PBS (pH 7.4) for 10 min at room temperature and washed again. The cells were permeabilized with 0.1% saponin for 10 min followed by incubation with 20 μM $SnCl_4$ dissolved in 100 μL DMEM at 37 °C for 1 h in a CO_2 incubator and observed under Andor spinning disk confocal microscope with excitation at 561 nm monochromatic laser beam. Images were recorded at emission wavelength between 630 and 650 nm. Metal treatment was followed by incubation in 10 μM probe in DMEM. After each treatment cells were washed three times with phosphate buffered saline (pH 7.4) to remove excess metal or probe. Again images were captured using EMCCD camera. In a separate coverslip undergoing the same treatment the cells were then treated with 30 μM of Na_2S solution for 1 h; the cells were washed with PBS three times to remove free compound and ions before analysis.

Prior to microscopic imaging, cells were fixed using 4% paraformaldehyde in PBS and washed, then all the solutions were aspirated and mounted on slides in a mounting medium containing DAPI (1 μg/mL) and stored in dark till the microscopic images are acquired.

MTT Cell Viability Assay. The cell viability was determined using a modified MTT assay. HCT cells were plated in 96-well micro assay culture plates (approximately 1×10^4 cells per well) and grown overnight at 37°C in a CO_2 incubator. To check the cytotoxic effect of **AR**, HCT 116 cells were seeded at tissue culture plate and incubated for 24 h at 37°C in CO_2 incubator. After incubation, 150μl of **AR** solution (0, 15, 25, 50, 75, and 100 μM), prepared in DMEM, was added to cells and the cultures were incubated for 24 hours. Solvent control samples (cells treated with DMSO in DMEM), no cells and cells in DMEM without any treatment were also included in the study. Four hours before the termination of experiment the growth media was removed, and 100μl DMEM containing MTT [3-(4,5-dimethylthiazol-2-yl)-2,5-diphenyltetrazolium bromide] (5 mg/ml) was added to the cells and incubated in CO_2 incubator at 37°C in dark for 4 hours. After incubation, the purple colored formazan produced in the cells appeared as dark crystals in the bottom of the wells. The insoluble colored formazan product was solubilized in DMSO producing a purple solution, and its absorbance was measured in a microtiter plate reader (Perkin-Elmer) at 570 nm. The assay was performed in triplicate for each concentration of **AR**, $SnCl_4$ and **AR**−$SnCl_4$ complex. The OD value of wells containing only DMEM medium was subtracted from all readings to get rid of the background influence. Data analysis and calculation of standard deviation was performed with Microsoft Excel 2007 (Microsoft Corporation).

Calculation for Association Constant Using Emission Titration Data. From the fluorescence titration data the association constant (K_a) for the formation of respective complex **AR**-Sn^{4+} was calculated by nonlinear curve fitting procedure. The non linear curve fitting was done using the following equation [2]

$$I = I_0 + \frac{I_{lim} - I_0}{2C_H}\left\{C_H + C_G + \frac{1}{K_a} - \left[\left(C_H + C_G + \frac{1}{K_a}\right)^2 - 4C_H C_G\right]^{1/2}\right\} \quad (1)$$

where I_0, I, and I_{lim} are the respective emission intensity of free **AR**, **AR** present in the form of [**AR**-Sn^{4+}] in the complex, and **AR** in presence of excess amounts of Sn^{4+} ions where the emission intensity reaches a limiting value. C_H and C_G are corresponding concentrations of host and cationic guest; K_a is the binding constant. The binding constant (K_a) and correlation coefficients (R) were obtained from a non-linear least-square analysis of I vs. C_H and C_G.

Detection Limit Calculation. The detection limit was calculated using emission titration data. The fluorescence emission spectrum of **AR** was measured by ten times, and the standard deviation of blank measurement was achieved. To gain the slope, the ratio of the fluorescence intensity at 582 nm was plotted as a concentration of Sn^{4+}. So the detection limit was calculated with the following equation [3]

$$\text{detection limit} = 3Sbl/S \quad (2)$$

where Sbl is the standard deviation of blank measurement and S is the slope of the calibration curve.

Computational Methods. Full geometry optimizations were carried out using the density functional theory (DFT) method at the B3LYP [4] level for the receptor (**AR**) and its Sn(IV) complex. All element except Sn were assigned 6-31+G(d) basis set. The LANL2DZ basis set with effective core potential (ECP) set of Hay and Wadt [5] was used for Sn. The vibrational frequency calculations were performed to ensure that the optimized geometries represent the local minima and there were only positive eigen values. Vertical electronic excitations based on B3LYP optimized geometry of the compounds were computed using the time-dependent density functional theory (TDDFT) formalism[6] in acetonitrile using conductor-like polarizable continuum model (CPCM)[7]. All calculations were performed with Gaussian09 program package[8] with the aid of the Gauss View visualization program.

2. ^{1}H NMR spectrum of AR (400 MHz, $CDCl_3$):

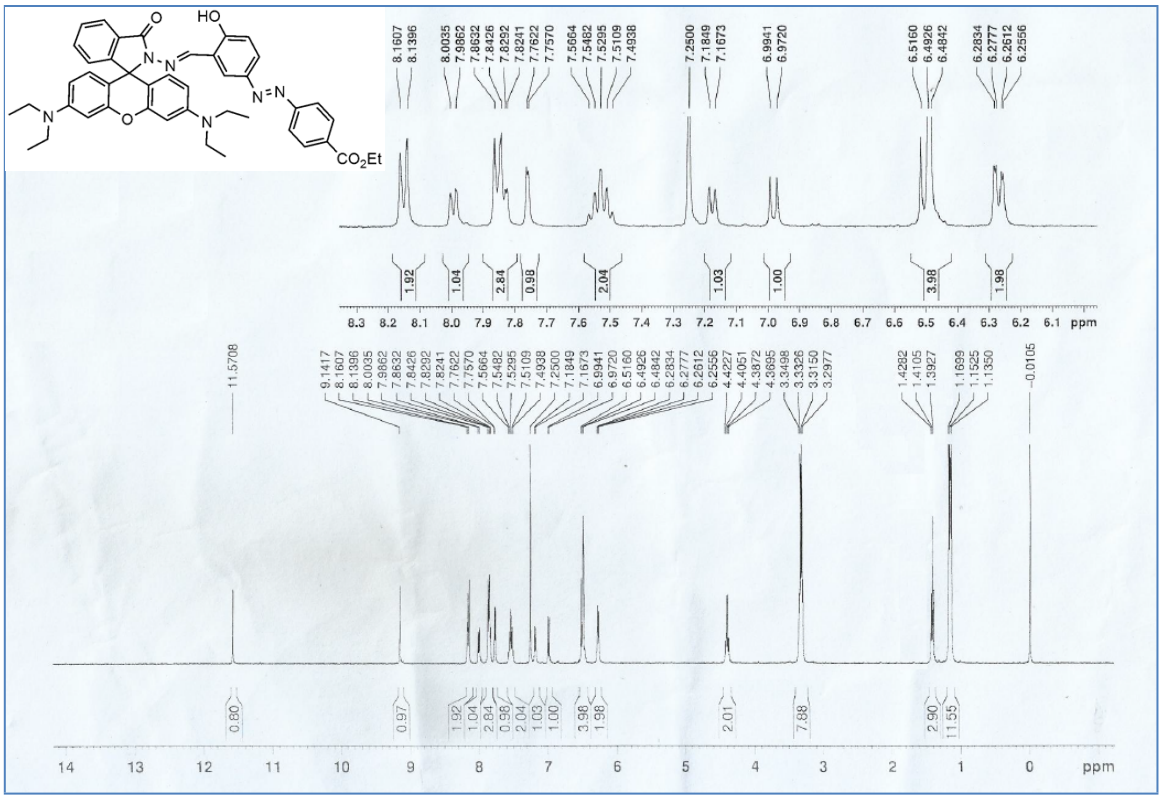

Figure S1: ^{1}H NMR spectrum of **AR** in $CDCl_3$ solution.

3.**^{13}C NMR spectrum of AR (400 MHz, $CDCl_3$):**

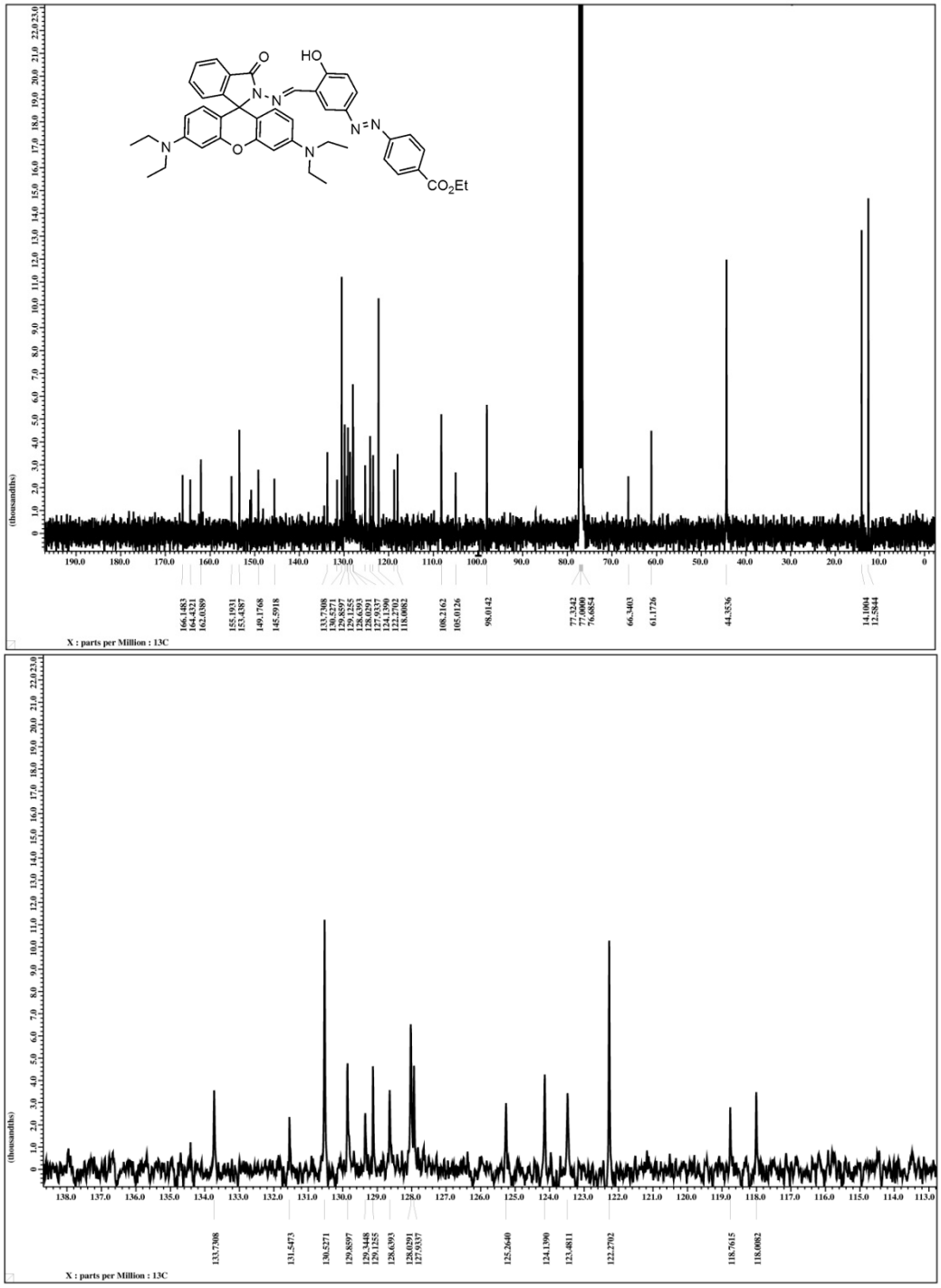

Figure S2: ^{13}C NMR spectrum of **AR** in $CDCl_3$ solution.

4. **TOF MS ES+ Mass Spectrum of AR:**

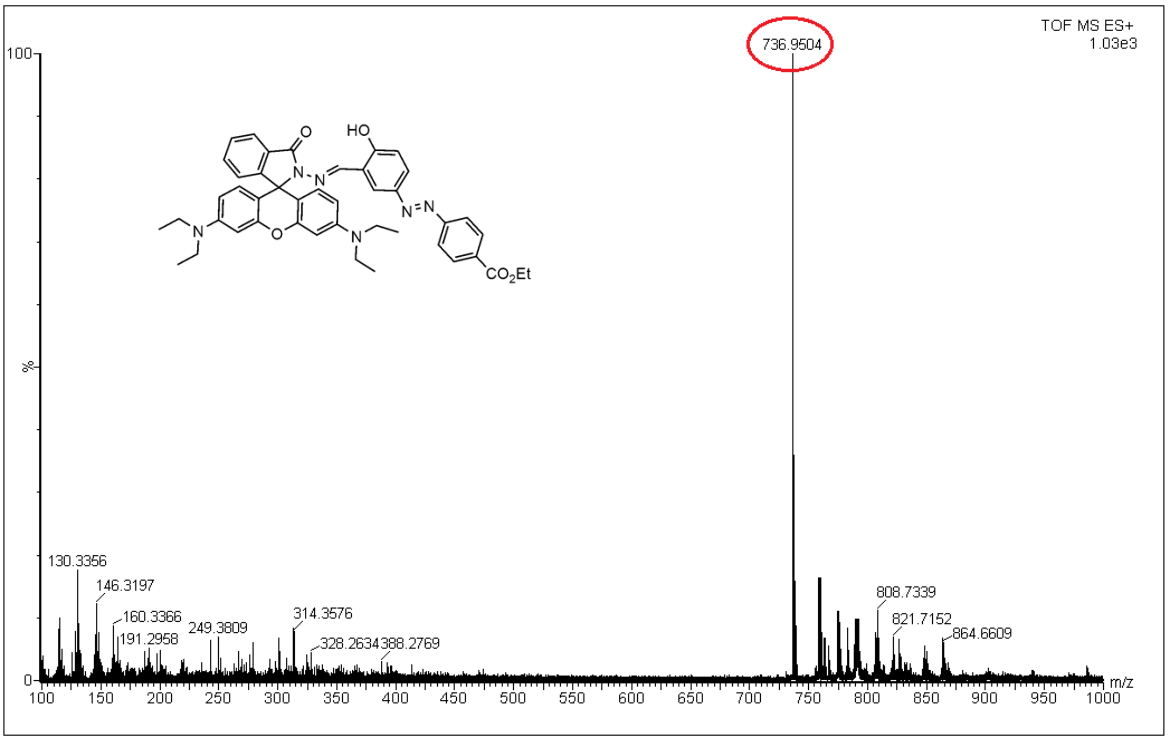

Figure S3: Mass spectrum of **AR** .

5. **TOF MS ES+ spectrum of AR in the presence $SnCl_4.5H_2O$:**

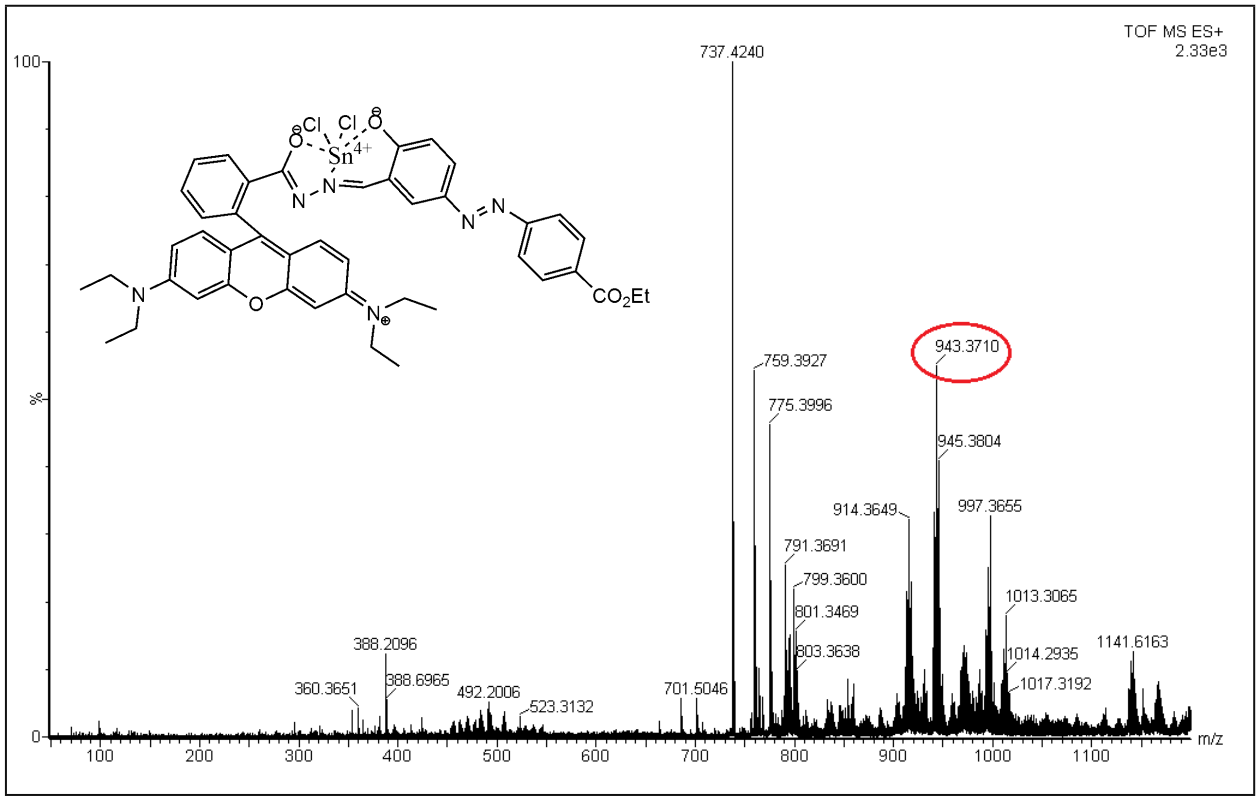

Figure S4: Mass spectrum of **AR**-Sn complex.

6. ^{1}H NMR spectrum of NAR (400 MHz, $CDCl_3$):

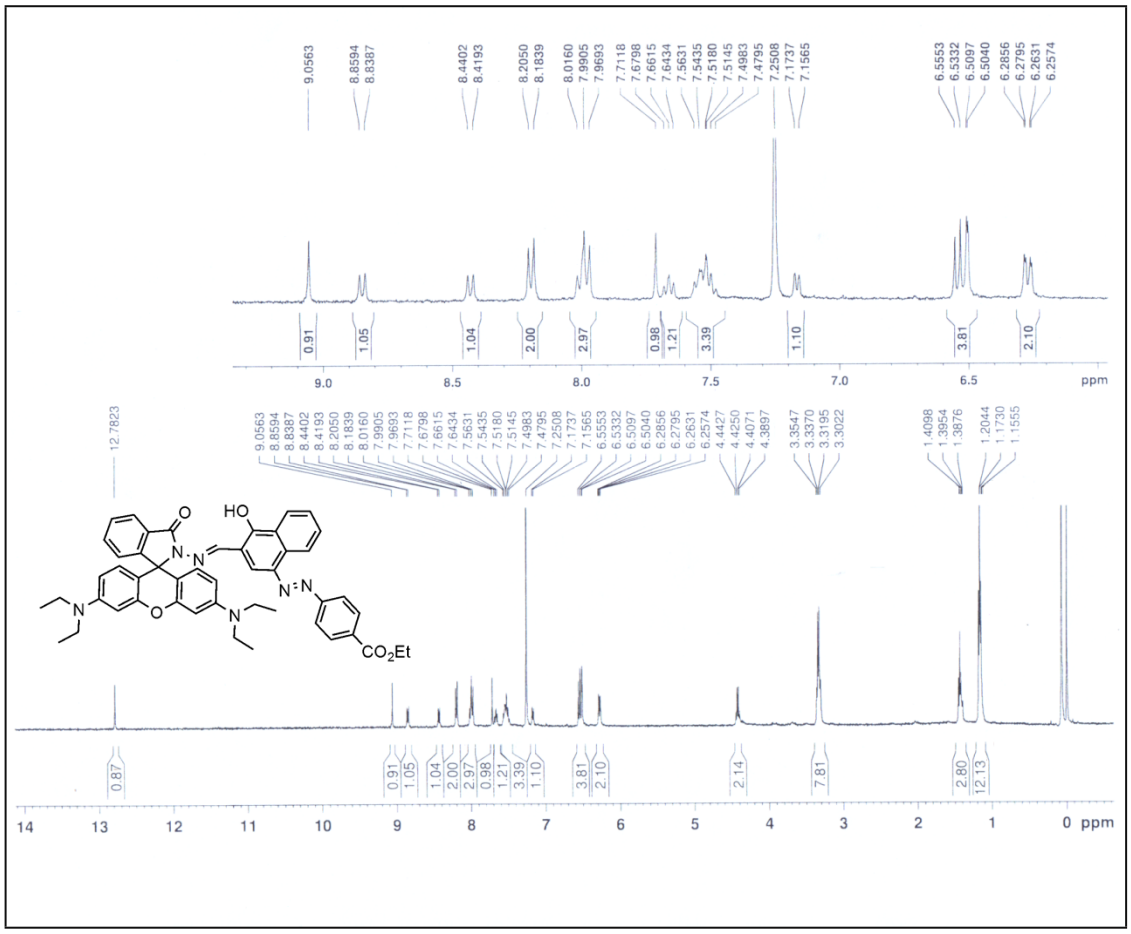

Figure S5: ^{1}H NMR spectrum of N**AR** in $CDCl_3$ solution.

7. **TOF MS ES+ Mass Spectrum of NAR:**

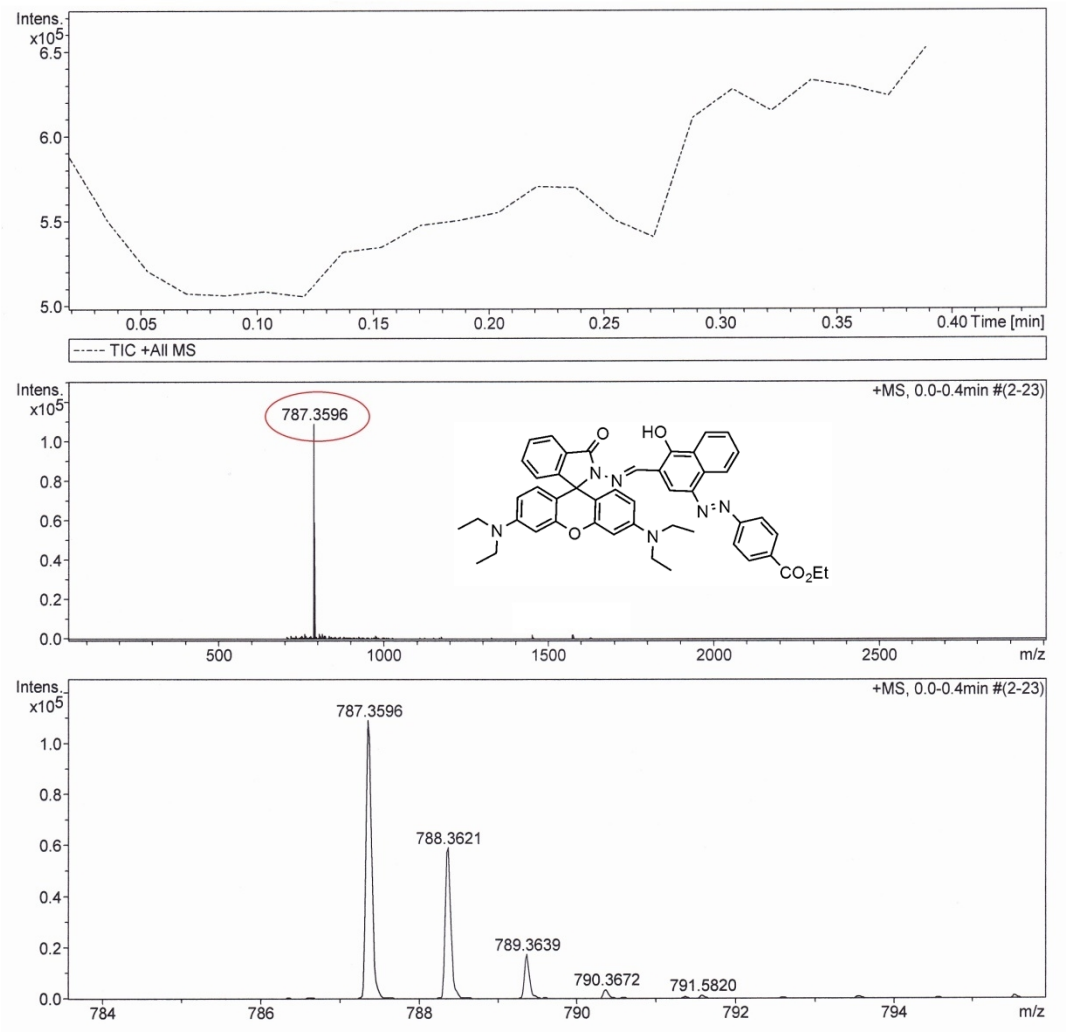

Figure S6: Mass spectrum of **NAR** .

8. **TOF MS ES+ spectrum of NAR in the presence $SnCl_4.5H_2O$:**

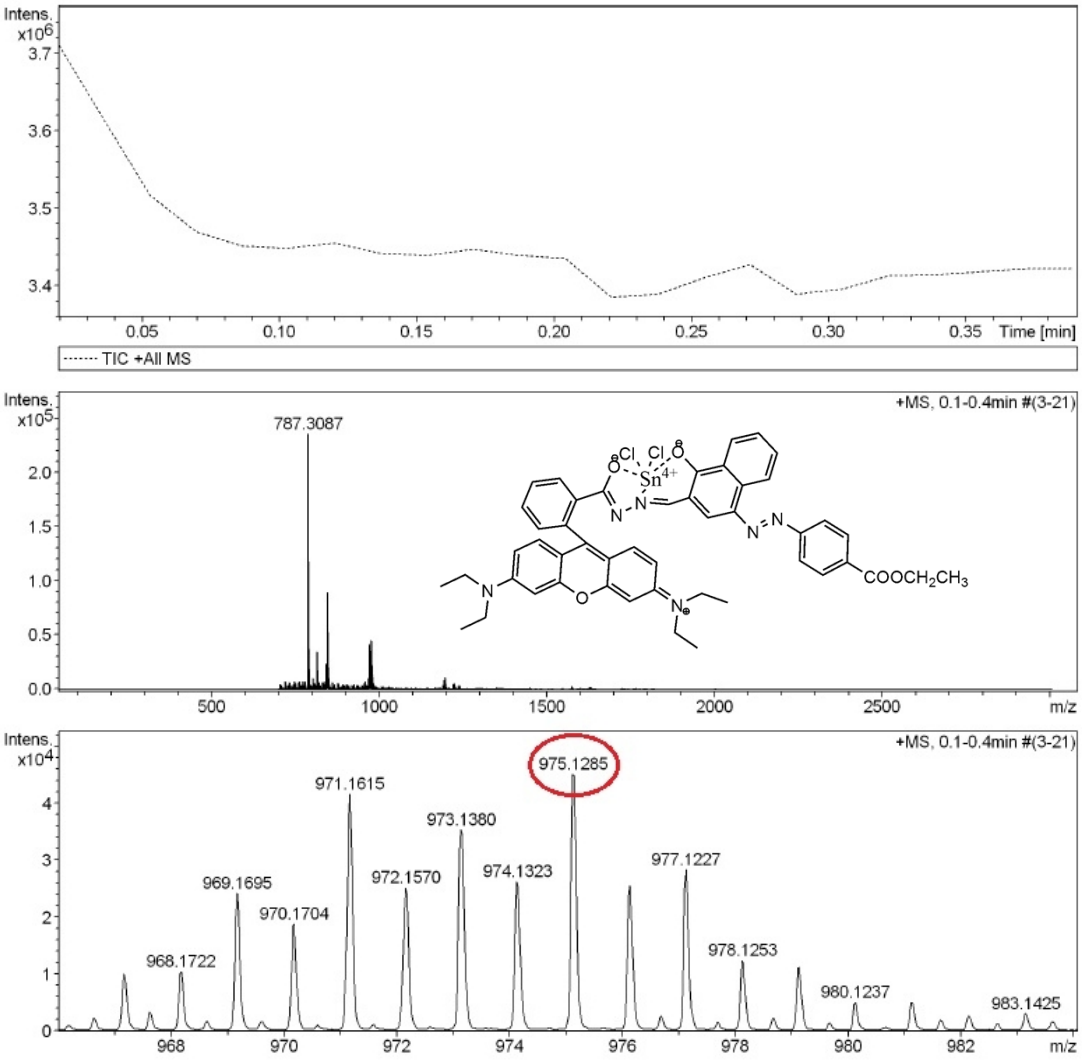

Figure S7: Mass spectrum of **NAR**-Sn complex.

9. Job's plot and association constant graph for AR-Sn^{4+}:

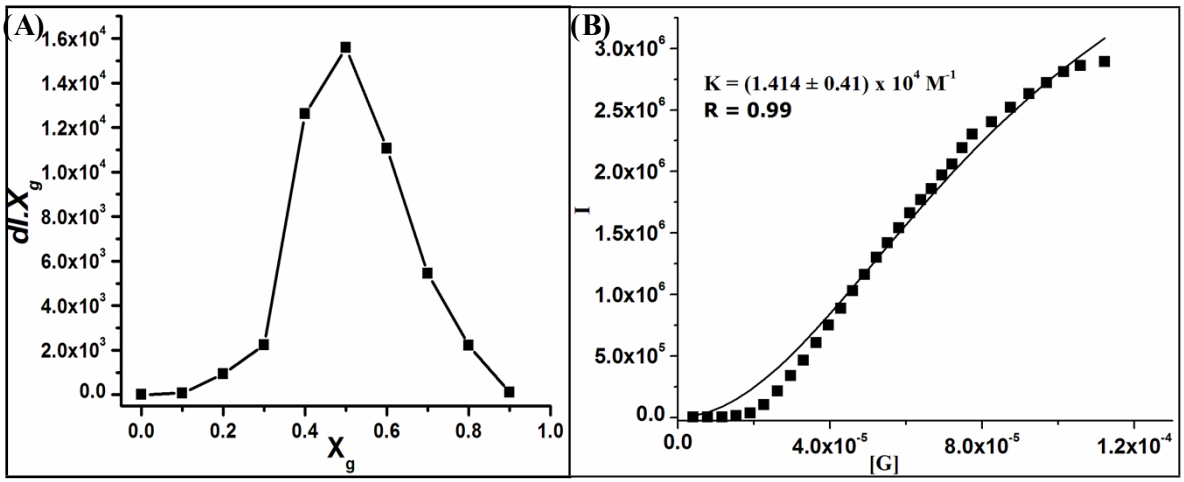

Figure S8. (A) Fluorescence Job's plot for **AR** with Sn^{4+} in EtOH–water (4: 1, v/v; 10 mM, HEPES buffer, pH = 7.4, ([H] = [G] = 4× 10^{-5} M). (B) Nonlinear curve fitting of the fluorescence titration data for **AR** (c = 4× 10^{-5} M) with Sn^{4+} (c= 4× 10^{-4} M) in EtOH / H_2O (4 : 1, v/v, 10 mM HEPES buffer, pH = 7.4).

10. FTIR spectra for AR and AR-Sn^{4+} :

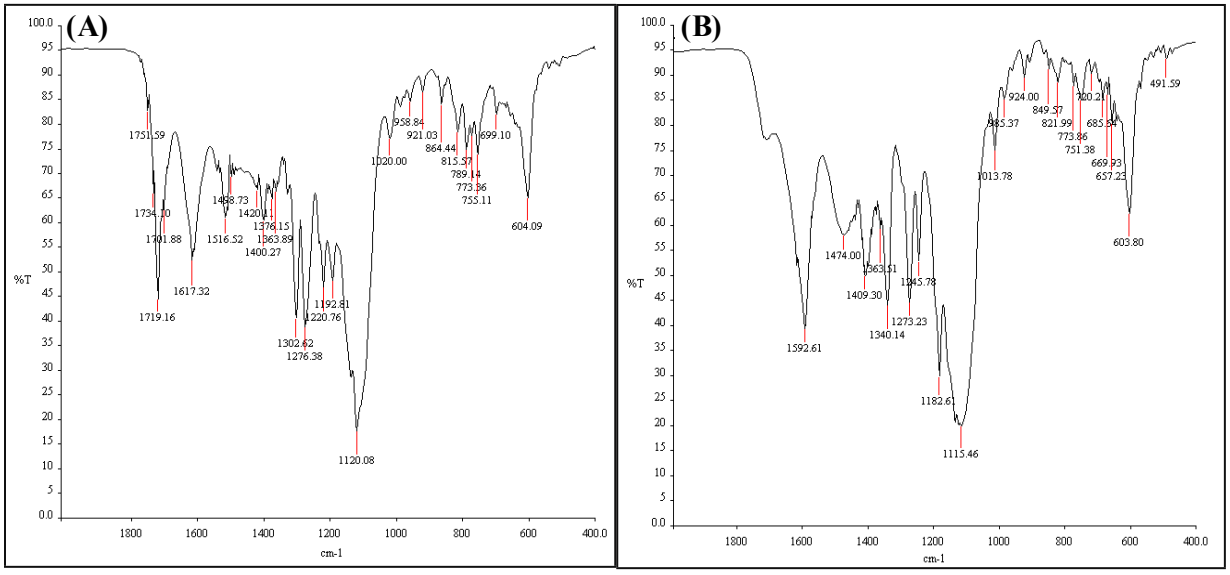

Figure S9. FTIR spectra of both (A) **AR** and (B) **AR**-Sn^{4+}.

11. Competitive experiments of AR:

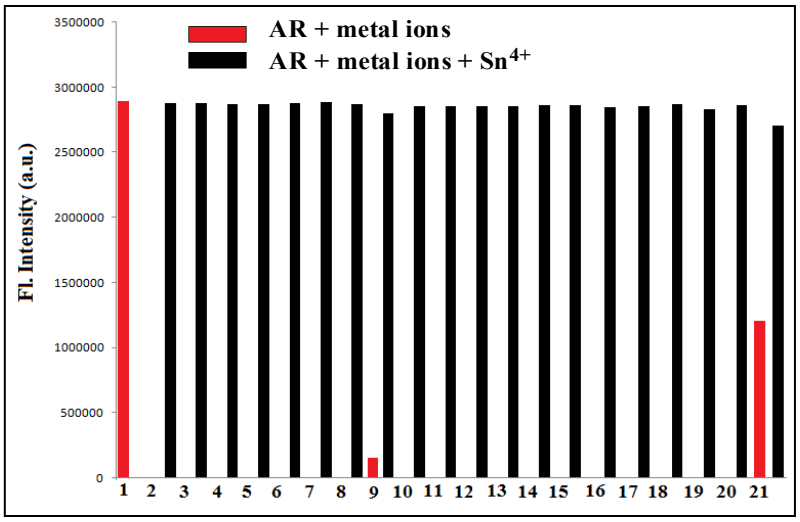

Figure S10. Fluorescence response of **AR** (c= 4× 10^{-5} M) to 4 eqv. addition of Sn^{4+} (c= 4× 10^{-4} M) and 10 eqv. of other metal ions (c= 4× 10^{-4} M) [the red bar portion] and to the mixture of 10 eqv. of other metal ions with 4 eqv. addition of Sn^{4+} [the black bar portion]. [Metal ions from 1 to 21: Sn^{4+}, Li^{+}, Na^{+}, K^{+}, Ca^{2+}, Mg^{2+}, Sr^{2+}, Ba^{2+}, Cr^{3+}, Mn^{2+}, Fe^{2+}, Fe^{3+}, Co^{2+}, Cu^{2+}, Ni^{2+}, Zn^{2+}, Cd^{2+}, Hg^{2+}, Pb^{2+}, Ag^{+} and Al^{3+}].

12. UV-vis Bar Diagram of AR in presence of various metal ions :

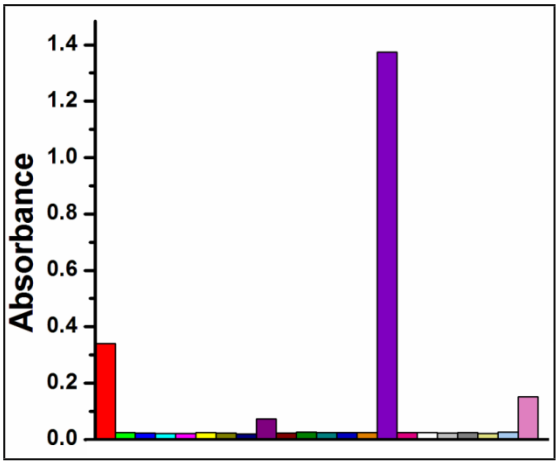

Figure S11. Change in the absorption spectrum of receptor **AR** [c = 4× 10^{-5} M, EtOH / H_2O = 4 : 1, v/v, 10 mM HEPES buffer, pH = 7.4) with respective metal cations (c = 4× 10^{-4} M, left to right- Sn^{4+}, AR, Li^{+}, Na^{+}, K^{+}, Ca^{2+} , Mg^{2+}, Sr^{2+}, Cr^{3+}, Ba^{2+}, Mn^{2+}, Fe^{2+}, Fe^{3+}, Co^{2+}, Cu^{2+}, Ni^{2+}, Zn^{2+}, Cd^{2+}, Hg^{2+}, Pb^{2+}, Ag^{+} and Al^{3+}).

13. Visual and fluorescence photographic image of AR in presence of different metal ions:

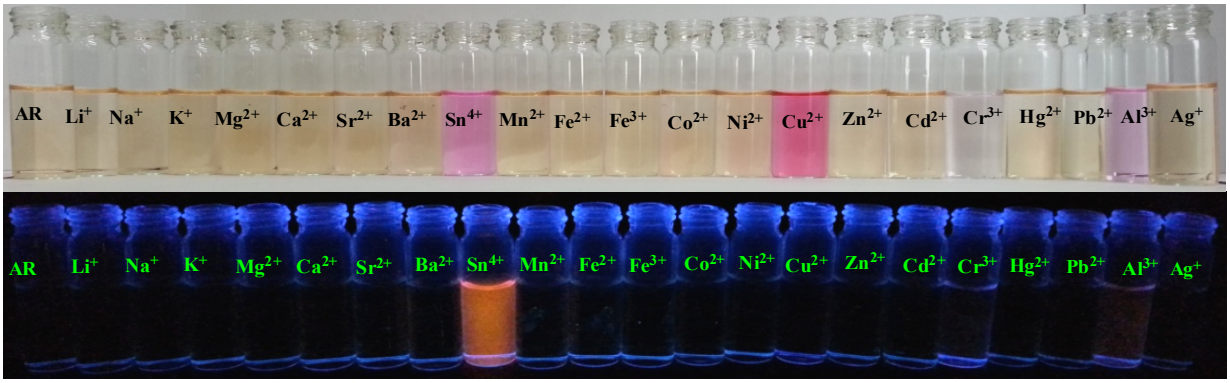

Figure S12: The Visible color (top) and fluorescence changes (buttom) of receptor **AR** in EtOH–H_2O solution (EtOH : H_2O = 4 : 1, v/v, 10 mM HEPES buffer, pH = 7.4) upon addition of various metal ions.

14. Reversibility Study:

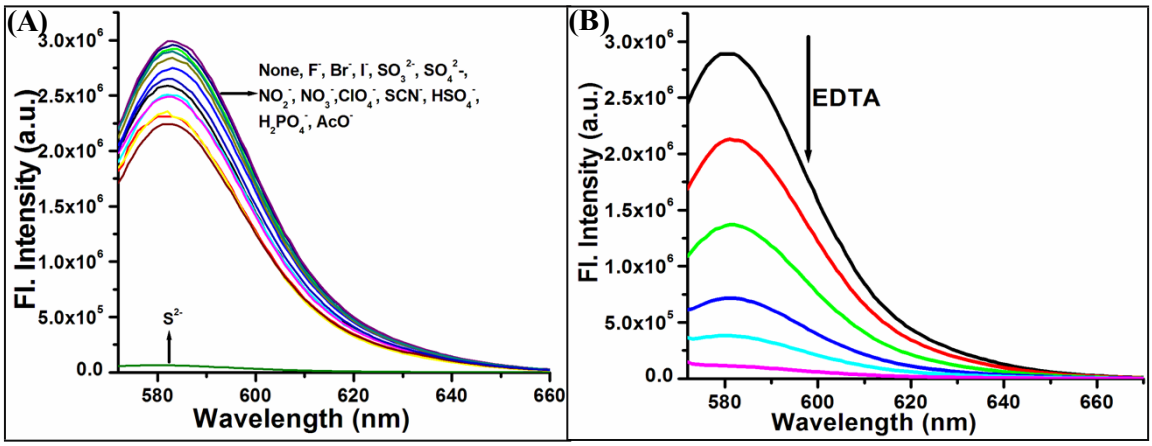

Figure S13: (A) Changes in the fluorescence spectra of **AR**−Sn complex in presence of different anions. (B) Change in fluorescence spectra of **AR**-Sn complex (c =4 x 10^{-5} M) in EtOH–H_2O solution (EtOH : H_2O = 4 : 1, v/v, 10 mM HEPES buffer, pH = 7.4) upon addition of Na_2EDTA (c = 4 x 10^{-4} M).

15. Absoption and emission spectra of NAR in presence of Sn^{4+} ions:

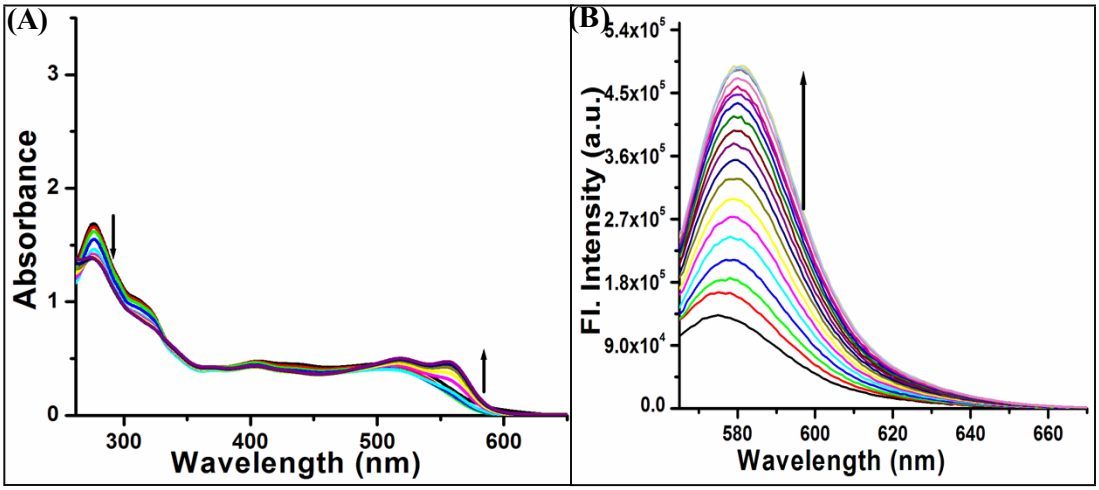

Figure S14: (A) Change in the absorption spectrum of receptor **NAR** [c = 4× 10^{-5} M, EtOH / H_2O = 4 : 1, v/v, 10 mM HEPES buffer, pH = 7.4) upon addition of increasing amounts of Sn^{4+} ions (c = 4× 10^{-4} M). (B) Change in the emission spectra of ligand **NAR** [c = 4× 10^{-5} M, EtOH / H_2O = 4 : 1, v/v, 10 mM HEPES buffer, pH = 7.4, λ_{ext}=563 nm) upon addition of Sn^{4+} ions (c = 4× 10^{-4} M).

16. **The effect of pH on the fluorescence intensity of AR and AR-Sn^{4+}:**

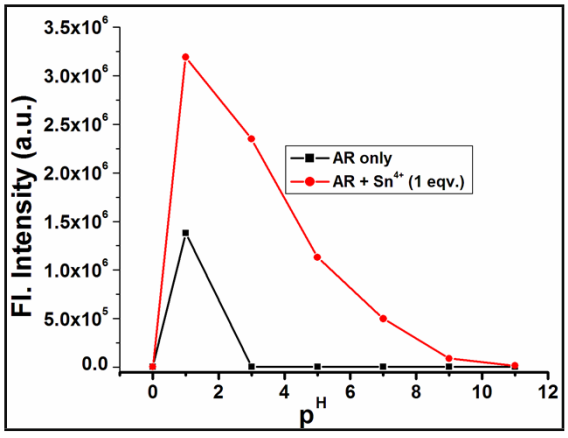

Figure S15: Fluorescence intensity of free chemosensor **AR** and in the presence of 1 equiv. Of Sn^{4+} in aq. EtOH (EtOH : H_2O = 4 : 1, v/v, 10 mM HEPES buffer, p^H=7.4) with different p^H conditions.

17. DFT Study:

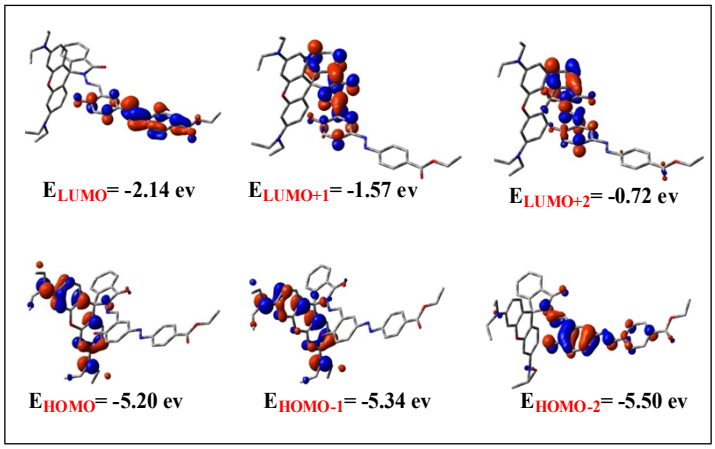

Figure S16. Contour plots of some selected MOs of the sensor **AR.**

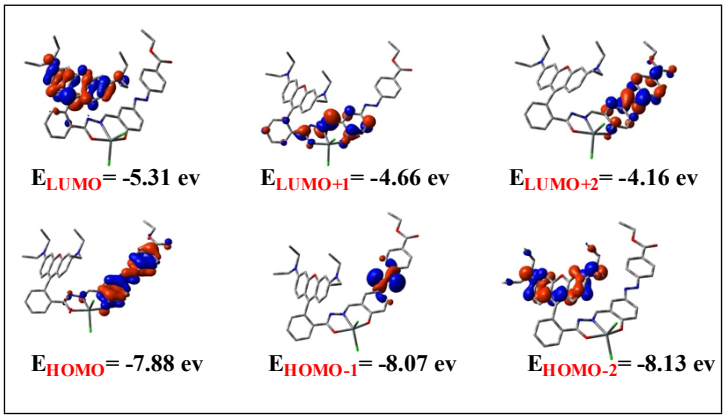

Figure S17. Contour plots of some selected MOs of the **AR**-Sn^{4+} complex.

Table S1. Selected vertical electronic transitions of **AR** calculated by TDDFT/CPCM method

$E_{excitation}$ (eV)	$\lambda_{excitation}$ (nm)	Osc. Strength (f)	Key transitions
2.9189	424.8	0.1017	(95%)HOMO→LUMO+1
2.9998	413.3	0.7236	(91%)HOMO-2→LUMO
3.4583	358.5	0.7473	(93%)HOMO-5→LUMO
3.4583	348.7	0.4472	(94%) HOMO-2→LUMO+1
4.1967	295.4	0.2224	(72%)HOMO-5→LUMO+1
4.5866	270.3	0.1226	(79%)HOMO-6→LUMO+1

Table S2. Selected vertical electronic transitions of **AR-Sn** complex calculated by TDDFT/CPCM method

$E_{excitation}$ (eV)	$\lambda_{excitation}$ (nm)	Osc. Strength (f)	Key transitions
2.3236	533.6	0.0445	(75%)HOMO→LUMO
2.9698	417.5	0.2197	(81%)HOMO-1→LUMO
3.0652	404.5	0.1047	(77%)HOMO-2→LUMO
3.2196	385.1	0.9060	(31%)HOMO-1→LUMO+2
			(31%)HOMO-1→LUMO+2
3.3106	374.5	0.2656	(65%)HOMO-2→LUMO+2
3.5785	346.5	0.2527	(79%)HOMO-4→LUMO+1
3.6560	339.1	0.3429	(76%)HOMO-5→LUMO

18. MTT assay:

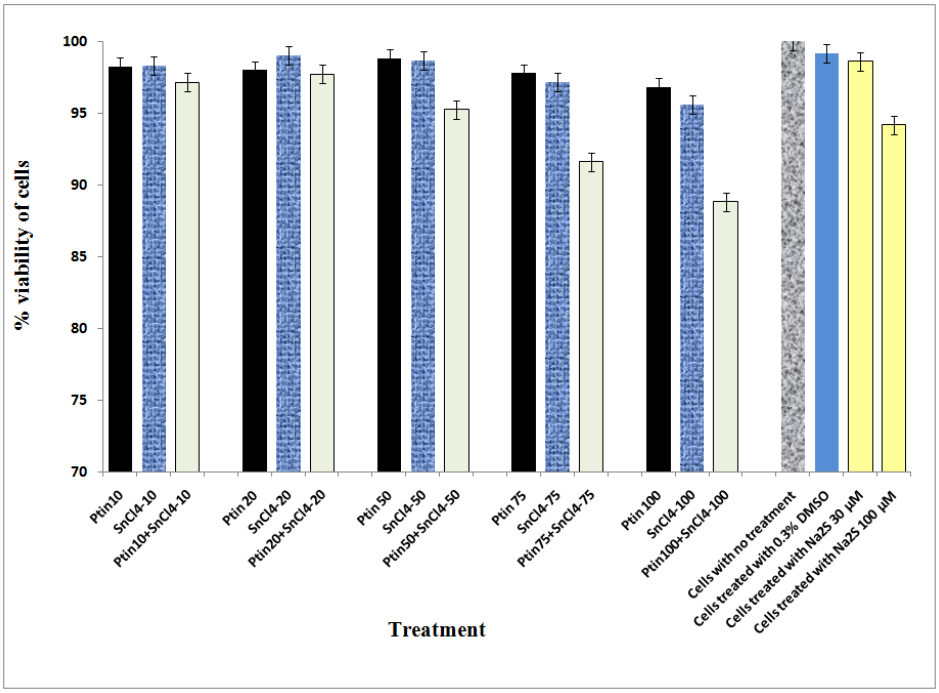

Figure S18. MTT assay to determine the cytotoxic effect of Probe **AR** and **AR**-Sn complex on HCT cells.

19. References:

1. Dujols, V.; Ford, F.; Czarnik, A. W. J. Am. Chem. Soc. **1997**, *119*, 7386-7387.

2. (a) Valeur, B.; Pouget, J.; Bouson, J. J. Phys. Chem. **1992**, *96*, 6545-6549. (b) Ghosh, K.; Sarkara, T.; Samadder, A. *Org. Biomol. Chem.* **2012**, *10*, 3236–3243.

3. (a) Long, L.; Zhang, D.; Li, X.; Zhang, J.; Zhang, C.; Zhou, L. *Anal. Chim. Acta* **2013**, *775,* 100–105. (b) Zhu, M.; Yuan, M., Liu, X.; Xu, J.; Lv, J.; Huang, C.; Liu, H., Li, Y.; Wang, S.; Zhu, D. *Org. Lett.* **2008**, *10*, 1481-1484. (c) Kar, C.; Adhikari, M. D.; Ramesh, A.; Das, G. *Inorg. Chem.* **2013**, *52*, 743−752.

4. (a) Becke, A. D. *J. Chem. Phys.* **1993**, *98*, 5648-5652. (b) Lee, C.; Yang, W.; Parr, R. G. *Phys. Rev. B* **1988**, **37**,785-789. (c) Andrae, D.; Haeussermann, U.; Dolg, M.; Stoll, H.; Preuss, H. *Theor. Chim. Acta* **1990**, *77*, 123-141.

5. (a) Hay, P. J.; Wadt, W. R. *J. Chem. Phys.* **1985**, *82*, 270-283. (b) Wadt, W. R.; Hay, P. J. *J. Chem. Phys.* **1985**, 82, 284-298. (c) Hay, P. J.; Wadt, W. R. *J. Chem. Phys.* **1985**, *82*, 299-310.

6. (a) Bauernschmitt, R.; Ahlrichs, R. *Chem. Phys. Lett.* **1996***,256*,454-464. (b) Stratmann, R. E.; Scuseria, G. E.; Frisch, M. J. *J. Chem. Phys.* **1998**, *109, 8218*-8224. (c) Casida, M. E.; Jamorski, C.; Casida, K. C.; Salahub, D. R. *J. Chem. Phys.* **1998**, *108*, 4439-4449.

7. (a) Barone, V.; Cossi, M. *J. Phys. Chem. A* **1998**, *102*,1995-2001. (b) Cossi, M.; Barone, V. *J. Chem. Phys.* **2001**, *115*, 4708-4717. (c) Cossi, M.; Rega, N.; Scalmani, G.; Barone, V. *J. Comput. Chem.* **2003**, *24*, 669-681.

8. Gaussian 09, Revision D.01, Frisch, M. J.; Trucks,G. W.; Schlegel, H. B.; Scuseria, G. E.; Robb, M. A.; Cheeseman, J. R.; Scalmani, G.; Barone, V.; Mennucci, B.; Petersson, G. A.; Nakatsuji, H.; Caricato, M.; Li, X.; Hratchian, H. P.; Izmaylov, A. F.; Bloino, J.; Zheng, G.; Sonnenberg, J. L.; Hada, M.; Ehara, M.; Toyota, K.; Fukuda, R.; Hasegawa, J.; Ishida, M.; Nakajima, T.; Honda, Y.; Kitao, O.; Nakai, H.; Vreven, T.; Montgomery, J. A.; Jr., Peralta, J. E.; Ogliaro, F.; Bearpark, M.; Heyd, J. J.; Brothers, E.; Kudin, K. N.; Staroverov, V. N.; Kobayashi, R.; Normand, J.; Raghavachari, K.; Rendell, A.; Burant, J. C.; Iyengar, S. S.; Tomasi, J.; Cossi, M.; Rega, N. Millam, J. M.; Klene, M.; Knox, J. E.; Cross, J. B.; Bakken, V.; Adamo, C.; Jaramillo, J.; Gomperts, R.; Stratmann, R. E.; Yazyev, O.; Austin, A. J.; Cammi, R.; Pomelli, C.; Ochterski, J. W.; Martin, R. L.; Morokuma, K.; Zakrzewski, V. G.; Voth, G. A.; Salvador, P.; Dannenberg, J. J.; Dapprich, S.; Daniels, A. D.; Farkas, Ö.; Foresman, J. B.; Ortiz, J. V.; Cioslowski, J.; Fox, D. J. Gaussian, Inc., Wallingford CT, 2009.